

Early diagenetic isotopic signal at the Cretaceous/Tertiary boundary, Israel

Mordechai Magaritz^a, Chaim Benjamini^b, Gerta Keller^c, Shimon Moshkovitz^d

^aDepartment of Environmental Sciences and Energy Research, Weizmann Institute of Science, Rehovot 76100, Israel and Division of Geological and Planetary Sciences, California Institute of Technology, Pasadena, CA 91125, USA

^bDepartment of Geology and Mineralogy, Ben Gurion University of the Negev, P.O. Box 653, Beer Sheva 84105, Israel

^cDepartment of Geological and Geophysical Sciences, Princeton University, Princeton, NJ 08544, USA

^dGeological Survey of Israel, Malkhei Yisrael 30, Jerusalem, Israel

(Received March 20, 1990; reviewed and accepted August 21, 1991)

ABSTRACT

Magaritz, M., Benjamini, C., Keller, G. and Moshkovitz, S., 1992. Early diagenetic isotopic signal at the Cretaceous/Tertiary boundary, Israel. *Palaeogeogr., Palaeoclimatol., Palaeoecol.*, 91: 291–304.

Carbon and oxygen isotope records from carbonate fractions in marls overlying the K/T boundary in southern Israel are used to interpret paleoenvironmental changes and the history of early diagenetic events in the earliest Tertiary. The $\delta^{13}\text{C}$ record of the whole rock does not significantly depart from the original values and reflects the global productivity drop shortly after the K/T boundary and the subsequent recovery. Fine fraction oxygen isotope values reflect the addition of carbonate cement highly depleted in ^{18}O throughout the profile. The $\delta^{18}\text{O}$ record demonstrates two main episodes in which contact with fresh water affected the sediments. One is below a short hiatus at planktic foraminiferal subzone transition PO/P1a (*Guembelitra cretacea*/Parvularugoglobigerina eugubina) and the other at an pyrite-rich clay layer near the top of planktic foraminiferal subzone P1b (*Globigerina taurica*). The latter event suggests introduction of sapropelic bottom conditions in the oceanic paleoenvironment.

Introduction

The most characteristic feature of the Cretaceous/Tertiary (K/T) $\delta^{13}\text{C}$ record is the negative excursion in the earliest Tertiary associated with a diminished surface-to-deep gradient and coincident with the elimination of many marine plankton species (Perch-Nielsen et al., 1982; Zachos and Arthur, 1986; Keller and Lindinger, 1989; Stott and Kennett, 1989; Barrera and Keller, 1990). The $\delta^{13}\text{C}$ signal is generally interpreted as a reduction of primary productivity in the oceans. Paleoenvironmental interpretations of the K/T boundary transition are primarily based on the $\delta^{13}\text{C}$ record because $\delta^{18}\text{O}$ compositions are many times more readily altered than $\delta^{13}\text{C}$ compositions due to the high concentration of oxygen and low concentration of carbon in diagenetic fluids in fine calcareous sediments (Magaritz, 1975, 1983).

Most K/T boundary stable isotopic records are based on whole rock and various fine fractions of the sediments, often with widely different results (Zachos and Arthur, 1986; Keller and Lindinger, 1989). Only a few studies are based on monospecific planktic and benthic foraminifera (Stott and Kennett, 1989; Barrera and Keller, 1990). This is largely because of early diagenetic alteration of foraminiferal test calcite, and disequilibrium effects of some species (Stott and Kennett, 1989). $\delta^{13}\text{C}$ values of fine fraction carbonate, which consists primarily of calcareous nannofossils, are also affected by diagenetic alteration and species compositional effects. Nevertheless, as with monospecific foraminifera, the environmental signal generally dominates these effects (Paull and Thierstein, 1987; Keller and Lindinger, 1989).

In the early Tertiary sections of southern Israel, patterns of environmental change have been inves-

tigated in planktic foraminifera, calcareous nannofossils, and changes in carbonate sedimentation (Keller et al., 1990; Keller and Benjamini, 1991). Stable isotope analyses of monospecific foraminifera has not been possible because of diagenetic alteration of sediments including recrystallization of fossil tests and redistribution of sedimentary carbonate which largely obscure the original climatic and environmental isotopic signal in these sections. However, some original environmental signal appears to be present in the patterns of redistribution of carbonate in the sediment which itself is the result of diagenetic events relevant to the post K/T history of the eastern Tethys. In this paper we attempt to identify the original isotopic signal and to reconstruct the early diagenetic history by tracing the redistribution of stable isotopes in several carbonate fractions.

More specifically, the goals of the present study are to analyze several size fractions in order (1) to identify those carbonate fractions in which the original isotopic signals were best preserved; (2) to trace the original isotopic excursions; and (3) to place them in a paleoenvironmental perspective. Where the isotopic signals were disturbed in one fraction in preference to another, the direction and magnitude of departure from original values may also be utilized to trace aspects of diagenetic history. In this way we can identify sedimentary surfaces affected by diagenesis in the early Paleocene. We will show that the isotopic signals correlate with hiatus intervals previously identified by planktic foraminiferal population studies in southern Israel (Keller et al., 1990; Keller and Benjamini, 1991). The magnitude of the effects will be suggestive of the intensity and duration of these events, while the isotope shifts will provide information on the types of fluids involved.

Geological background

Keller et al. (1990) found the early Tertiary sedimentary sequence in the eastern Tethys to be punctuated by widespread events of erosion and nondeposition. One of the sections studied was at the base of the Taqiye Formation, exposed some 100 km southwest of Beer Sheva near the Sinai border in the Negev, Israel. There, the upper part

of the Cretaceous Ghareb Formation is composed of a marly chalk consisting of some 90% CaCO_3 . Carbonate content gradually drops to 50–60%, with a downward spike to 40% at a black clay horizon positioned 2.6 m above the K/T boundary. Thereafter, carbonate increases gradually to 60% and fluctuates around this mean to the top of the studied section. The lower 60 cm of the Taqiye Formation is mottled with flakes of reworked Maastrichtian chalk embedded in Tertiary grey clay. Bioturbation and mottling decreases up-section although *Chondrites* burrows can be observed.

Clays in the Taqiya Formation of the Negev have been analyzed by Nathan (1969) and Arkin et al. (1972). At the base of the Taqiya Formation, the clay fraction consists of 40–60% montmorillonite, 30–50% kaolinite, and 10–20% illite. Disseminated pyrite lends a dark grey color to the clays, and pyritic concretions, usually oxidized, and gypsum veining, is common. At least 90% of the CaCO_3 is in the $< 32 \mu\text{m}$ fraction, and SEM inspection has shown that the carbonate fraction is entirely composed of coccoliths. The 32–64 μm fraction is composed of some 95% planktic foraminifers, with about 5% small benthic foraminifers, thoracosphaerids (calcareous dinocysts) and indeterminate biogenic debris. The $> 63 \mu\text{m}$ fraction is quantitatively unimportant, being $< 1\%$ of the bulk, with P/B ratios $> 90\%$ except near the K/T boundary itself.

The section was zoned biostratigraphically by planktic foraminifera and calcareous nannofossils, and the part of the section presented here was found to represent about 300,000 to 400,000 years at the base of the Tertiary. No clear sedimentary breaks can be observed in the field, but sedimentary hiatuses were identified by abrupt changes in the planktic foraminiferal populations, particularly at zonal boundaries (Keller et al., 1990). Smaller benthic foraminiferal populations were characteristic of a "Midwayan" assemblage, indicating outer continental shelf to upper slope environments (Keller, 1990). In most sections in the Negev, a characteristic horizon of black clay a few centimeters thick, rich in pyrite and with low P/B foraminiferal ratios, is found some meters above the K/T boundary in the upper part of foraminiferal subzone P1b (biostratigraphy after Keller and Benjamini, 1991).

In the Sinai section this interval was located 2.6 m above the K/T boundary.

Materials and methods

The outcrop section is located in the western Negev desert of Israel, about 50 km SW of Beer Sheva (Fig.1). The section is located on a steep (30–40°) slope, and samples were taken from a

30–50 cm deep trench to eliminate surface contamination. Sampling was at 5–10 cm vertical intervals near the boundary and 50 cm intervals upwards. For this study, three types of material were used: whole rock samples (w.r.), total material finer than 63 μm (< 63 μm), and a sample from the 63–32 μm fraction. The three fractions were analyzed for carbon and oxygen isotopes according to the analytical methods outlined in Magaritz et al. (1985).

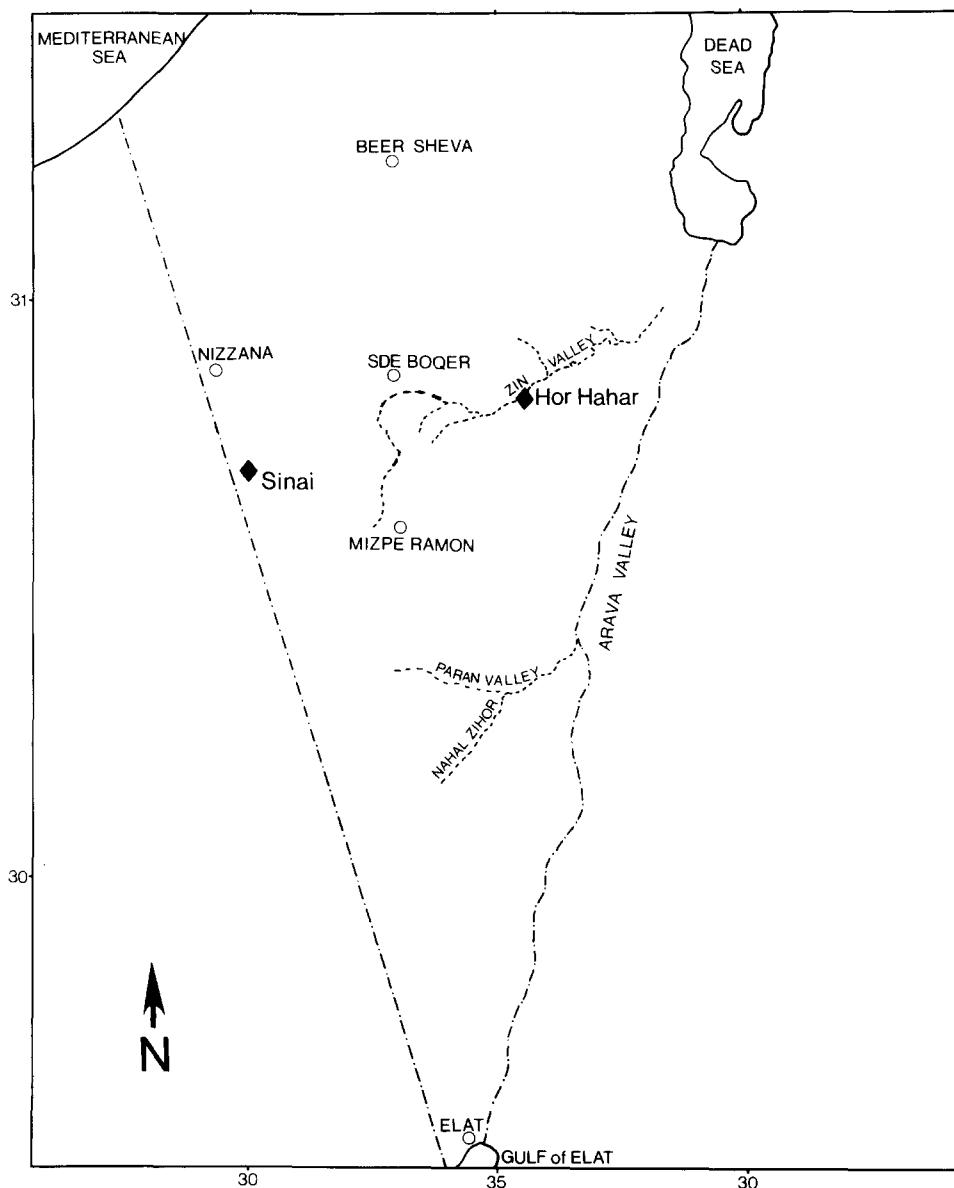


Fig.1. Negev location map showing the Sinai Border section as well as the Hor HaHar section studied earlier by Magaritz et al. (1985). Sampled localities are marked by black diamonds.

The same samples were used for quantitative planktic foraminiferal analysis and percent carbonate, as reported by Keller et al. (1990), and benthic foraminifera, organic matter and calcareous nanofossils are under study. Although preservation was good enough for biostratigraphic analysis, individual planktic foraminifera are recrystallized, have calcitic infillings and overgrowths, making them unsuitable for monospecific isotopic studies. On the other hand, the calcareous nanofossils, lacking body cavities, seem to be less altered by CaCO_3 crystal growth.

Results

Carbon isotope data

The carbon isotope values for the three studied sediment fractions from the Sinai border section are shown in Fig.2 and Table 1. All three $\delta^{13}\text{C}$ isotope profiles show very similar trends, but the magnitude of change is greater in the whole rock (w.r.) and $< 63 \mu\text{m}$ fraction than in the $63\text{--}32 \mu\text{m}$ fraction. The difference between the $\delta^{13}\text{C}$ isotopic values in the w.r. samples and the two fine fractions

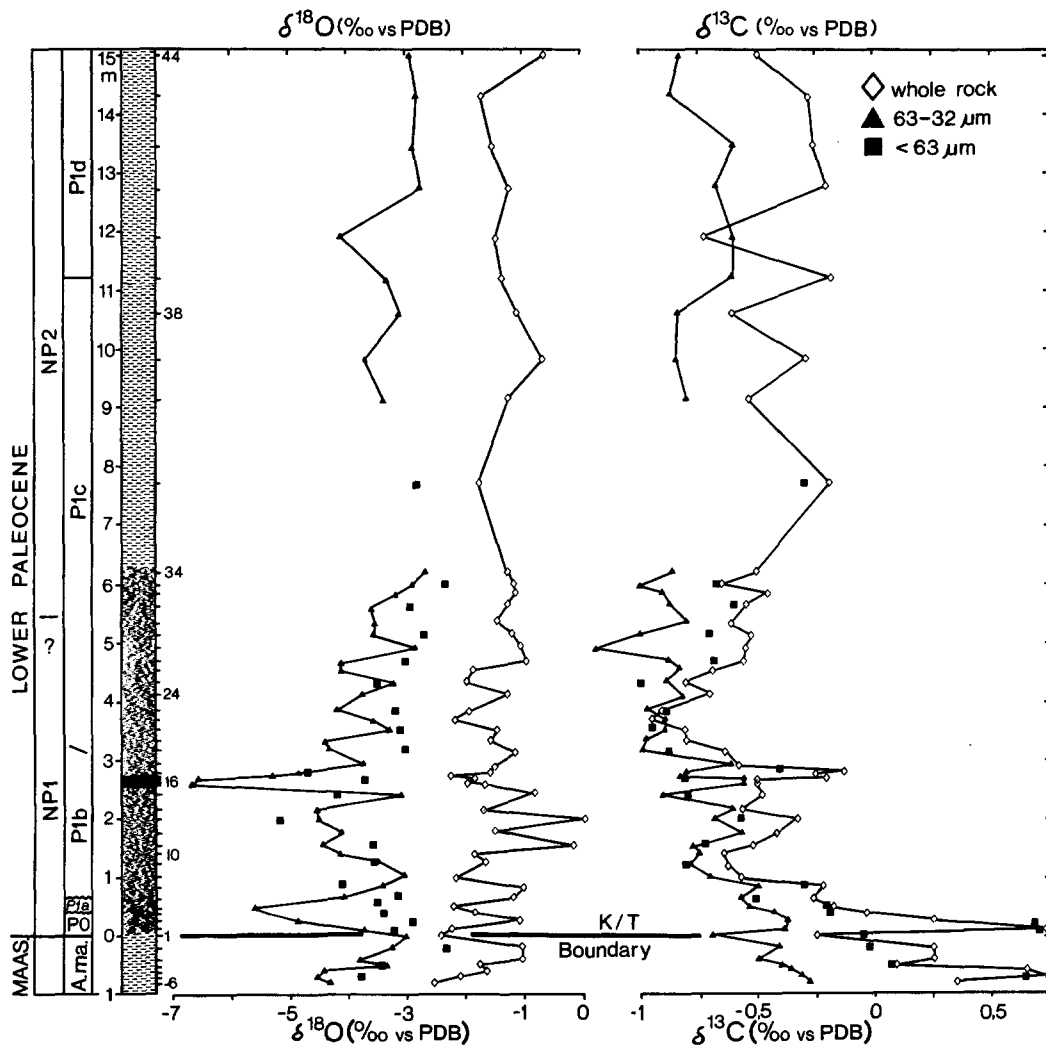


Fig.2. Carbon and oxygen isotopic profiles of the whole rock and two fine fractions from the Sinai Border section. Stratigraphy after Keller et al. (1990). Stratigraphic column emphasizes calcareous marls below K/T, mottled marl at and above the boundary, black clay horizon at P1b/P1c transition, and calcareous marls from P1c. Lithological distinctions are more subtle in the field.

TABLE 1

Carbon and oxygen isotope measurements of whole rock and fine fractions in the Sinai border section

Sample no.	Depth (m)	Whole rock		Fine fraction (< 63 μm)		Fine fraction (63–32 μm)	
		$\delta^{18}\text{O}$ (‰)	$\delta^{13}\text{C}$ (‰)	$\delta^{18}\text{O}$ (‰)	$\delta^{13}\text{C}$ (‰)	$\delta^{18}\text{O}$ (‰)	$\delta^{13}\text{C}$ (‰)
–6	–0.54	–2.57	0.35	–4.33	–0.28		
–5	–0.46	–2.09	0.73	–4.54	–0.31	–3.81	0.64
–4	–0.41	–1.63	0.65	–4.42	–0.36		
–3	–0.40	–1.78	0.09	–3.34	–0.38	–3.43	0.07
–2	–0.34	–1.03	0.25	–3.80	–0.51		
–1	–0.01	–1.04	0.25	–3.28	–0.42	–2.33	–0.03
1	0.00	–2.43	–0.25	–3.03	–0.71	–3.01	–0.04
2	0.12	–2.24	0.71	–3.76	–0.38	–3.23	0.70
3	0.26	–1.07	0.25	–4.86	–0.36	–2.94	0.69
4	0.39	–1.88	–0.04	–5.37	–0.43	–3.40	–0.20
5	0.47	–2.22	–0.18	–5.64	–0.54	–3.52	–0.20
6	0.66	–1.20	–0.27	–4.09	–0.58	–3.15	–0.52
7	0.86	–1.00	–0.22	–3.47	–0.49	–4.10	–0.30
8	1.03	–2.17	–0.58	–3.03	–0.71		
9	1.22	–1.63	–0.63	–3.48	–0.79	–3.53	–0.79
10	1.40	–1.87	–0.65	–4.14	–0.71		
11	1.56	–0.15	–0.53	–4.45	–0.78	–3.58	–0.73
12	1.73	–1.52	–0.44	–4.12	–0.57		
13	2.00	0.02	–0.33	–4.56	–0.69	–5.21	–0.57
14	2.16	–1.68	–0.57	–4.55	–0.62		
15	2.42	–0.80	–0.48	–3.07	–0.92	–4.21	–0.79
16a	2.59	–1.58	–0.50	–6.71	–0.56		
16b	2.60	–1.99	–0.50	–4.41	–0.79	–3.69	–0.83
16c	2.61	–1.82	–0.21	–6.57	–0.55		
16d	2.63	–2.26	–0.25	–5.30	–0.84		
17	2.87	–1.59	–0.14	–4.84	–0.80	–4.70	–0.40
18	2.93	–1.50	–0.58	–3.73	–0.61		
19	3.18	–1.12	–0.64	–4.37	–1.01	–3.01	–0.88
20	3.36	–1.58	–0.81	–4.43	–0.97		
21	3.52	–1.42	–0.82	–3.32	–0.89	–3.10	–0.94
22	3.70	–2.17	–0.95	–3.58	–0.88		
23	3.88	–1.93	–0.91	–4.18	–0.97	–3.20	–0.98
24	4.13	–1.29	–0.70	–3.75	–0.82		
25	4.34	–1.99	–0.82	–3.25	–0.88	–3.51	–0.99
26	4.56	–1.88	–0.69	–4.14	–0.82		
27	4.70	–0.92	–0.57	–4.14	–0.87	–3.00	–0.68
28	4.93	–1.04	–0.57	–2.84	–1.19		
29	5.15	–1.20	–0.52	–3.59	–1.01	–2.70	–0.71
30	5.36	–1.46	–0.62	–3.53	–0.79		
31	5.63	–1.27	–0.54	–3.60	–0.88	–2.94	–0.60
32	5.84	–1.12	–0.46	–3.19	–0.90		
33	5.97	–1.15	–0.65	–2.92	–0.99	–2.36	–0.66
34	6.20	–1.28	–0.50	–2.70	–0.86		
35	7.70	–1.78	–0.18			–2.81	–0.30
36	9.13	–1.27	–0.53	–3.43	–0.80		
37	9.81	–0.63	–0.28	–3.71	–0.85		
38	10.61	–1.10	–0.60	–3.12	–0.85		
39	11.20	–1.38	–0.17	–3.34	–0.60		
40	11.92	–1.49	–0.72	–4.13	–0.60		
41	12.74	–1.25	–0.19	–2.74	–0.67		
42	13.46	–1.52	–0.26	–2.89	–0.61		
43	14.30	–1.71	–0.28	–2.79	–0.88		
44	15.00	–0.60	–0.49	–2.95	–0.83		

are illustrated in Fig. 3. For the total fine fraction ($<63 \mu\text{m}$) most of the $\delta^{13}\text{C}$ values are less than 0.3‰ with a mean value 0.11‰ . In only two samples is the fine fraction enriched relative to w.r. values. These two samples are within the PO (*Guembeltria cretacea*) interval at the K/T boundary. At the pyrite-rich dark clay layer 2.6–2.7 m above the K/T boundary in the uppermost part of Zone P1b a $\delta^{13}\text{C}_{\text{w.r.} - <63 \mu\text{m}}$ maxima occurs.

In contrast, the $63\text{--}32 \mu\text{m}$ fraction, which is composed primarily (95%) of very small planktic foraminifera (Fig. 4), shows larger deviations relative to w.r. values with a $\delta^{13}\text{C}_{\text{w.r.} - (63\text{--}32) \mu\text{m}}$ mean of 0.36‰ . The largest deviation, up to 1.0‰ , was found in the ^{13}C enriched intervals in the upper-

most Maastrichtian and in Zone P0 and the smallest deviation occurs in the $\delta^{13}\text{C}$ minima zone 3.5–4.5 m above the K/T boundary. Relatively large $\delta^{13}\text{C}_{\text{w.r.} - (63\text{--}32) \mu\text{m}}$ fluctuations occur in the lower part of the section where samples with no significant faunal difference alternate with $\delta^{13}\text{C}$ values of 0.5‰ .

Despite these differences in $\delta^{13}\text{C}$ values of the three fractions, the overall trends in the $\delta^{13}\text{C}$ values are very similar and seem to record changing environmental conditions. In the uppermost Maastrichtian sediments there is a 0.5‰ negative change in the $63\text{--}32 \mu\text{m}$ fraction and a 1.0‰ negative change in the w.r. and $<63 \mu\text{m}$ fractions reaching minimum values at the K/T boundary,

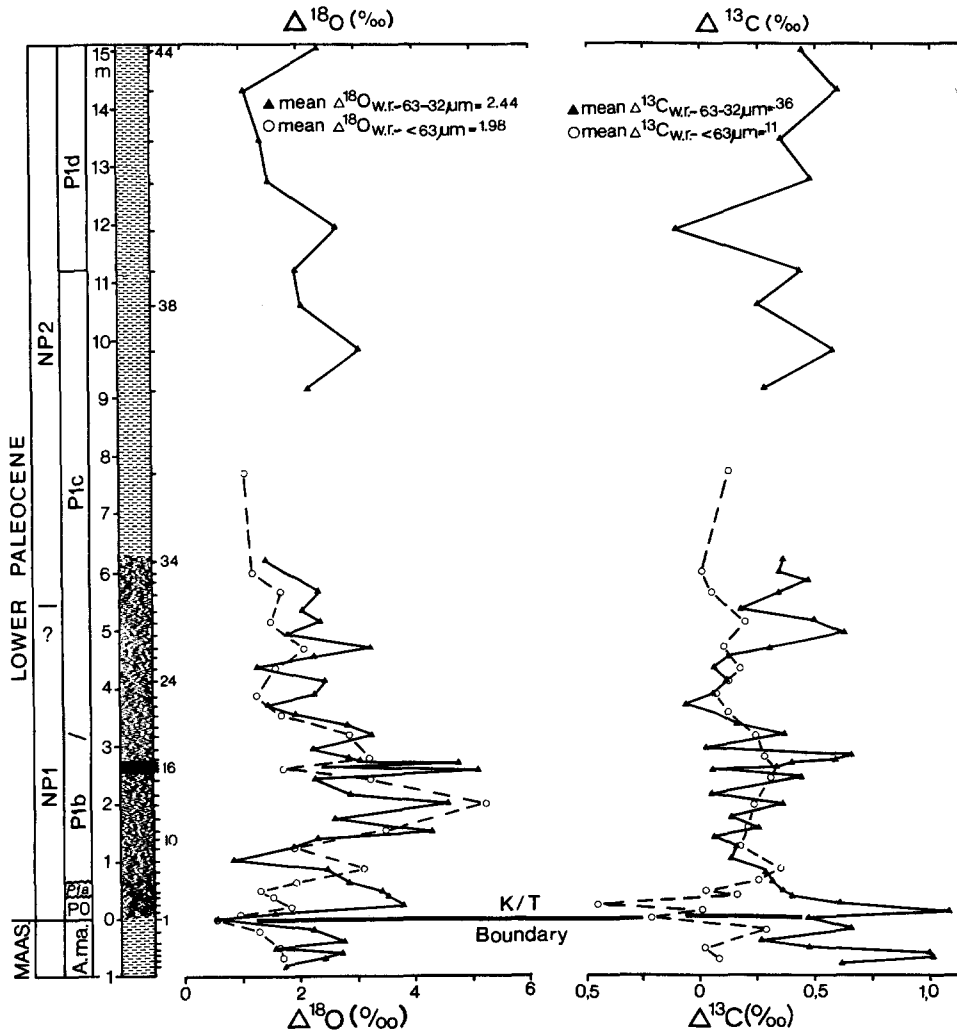


Fig. 3. Isotopic composition difference ($\delta^{13}\text{C}$ and $\delta^{18}\text{O}$) between whole rock values and the two separated fine fractions.

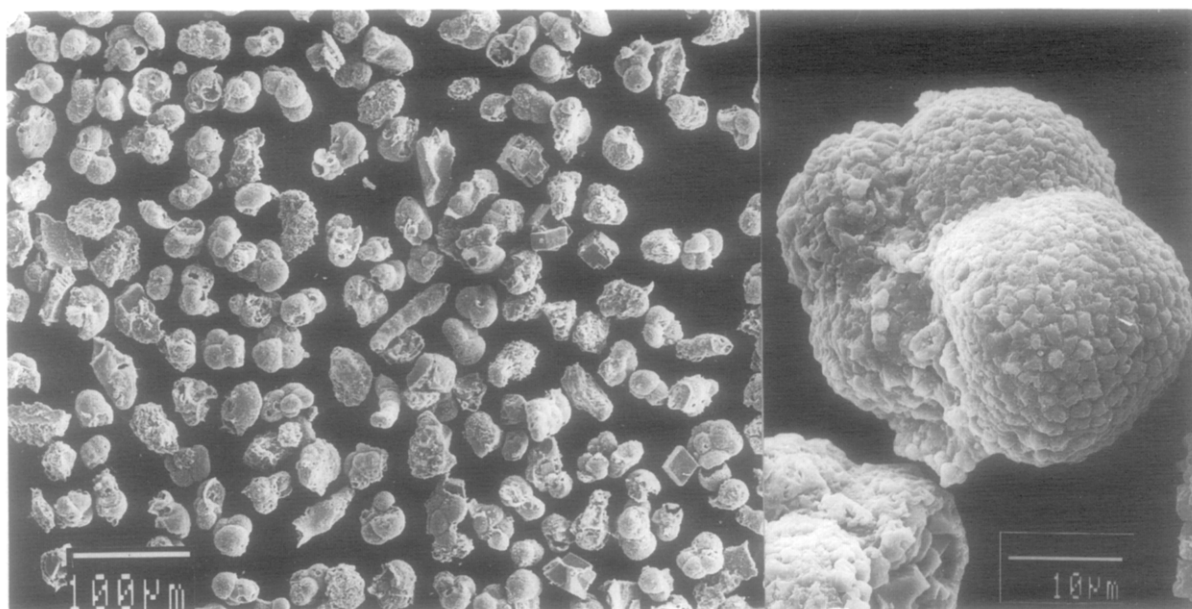


Fig. 4. SEM photos of the 63–32 μm fraction showing carbonate cement overgrowths on original test material of planktic foraminifera. Addition of carbonate cement significantly affects $\delta^{13}\text{C}$ and $\delta^{18}\text{O}$ of this fine fraction. Material shown is from sample S-5, zone P1a, at K/T+0.5 m.

In the basal Danian planktic foraminiferal Zone P0, $\delta^{13}\text{C}$ values of the 63–32 μm fraction rise 0.5‰ and 1.0‰ in w.r. and <63 μm fractions. However, because the basal Tertiary dark grey clay includes reworked tan-coloured clasts from the Cretaceous, part or all of this $\delta^{13}\text{C}$ excursion may represent Cretaceous values (Keller et al., 1990).

In Zone P0, $\delta^{13}\text{C}$ values drop sharply, and reach temporary minimum values between P0/P1a and P1a/P1b Subzone boundaries. These planktic foraminiferal zone boundaries are characterized by the sudden appearance and equally sudden disappearance of large numbers of two short ranging species (*Parvularugoglobigerina eugubina* and *Globastica comusa*, Fig. 5). Such sudden truncation of abundant individuals generally indicates the presence of a short hiatus. In the Sinai border section we interpret the faunal record to indicate the presence of two short hiatuses at the planktic foraminiferal Zone and Subzone P0/P1a and P1a/P1b boundaries. These hiatuses are also implied by the very short Subzone P1a interval (Keller et al., 1990) as compared to sections at El Kef, Brazos River, Caravaca and Agost (Smit, 1982; Keller, 1988, 1989a,b; Canudo, 1990).

At the P1a/P1b Subzone boundary, $\delta^{13}\text{C}$ values decrease further, and remain relatively low during Zone P1b between 1.0 m and 2.6 m above the K/T boundary. Interestingly, the opportunistic Cretaceous survivor *Guembeltria* (mainly *G. cretacea* and *G. trifolia*) reaches maximum abundance (~60%) during this low $\delta^{13}\text{C}$ interval. Between 2.6 m and 2.7 m a sharp 0.5‰ rise in $\delta^{13}\text{C}$ values occurs within a 10–12 cm thick black pyrite rich clay layer. *Guembeltria* species abundances decline dramatically at this interval (<10%) and disappear shortly thereafter (Fig. 5). $\delta^{13}\text{C}$ minimum values are reached between 3 m and 4.5 m above the K/T boundary near the planktic foraminiferal P1b/P1c Subzone boundary and nannofossil NP1/NP2 Zone boundary (Fig. 2). This interval of low $\delta^{13}\text{C}$ values is followed by a gradual 1.0‰ increase in w.r. and <63 μm fraction values. Generally higher, but variable $\delta^{13}\text{C}$ values characterize the upper part of the section (Subzones P1c and P1d, Fig. 2). The 63–32 μm fraction shows smaller variations in the $\delta^{13}\text{C}$ curve but the values remain low to the top of the section. Coincident with increasing $\delta^{13}\text{C}$ values is the appearance and increasing abundance of two planktic foraminiferal

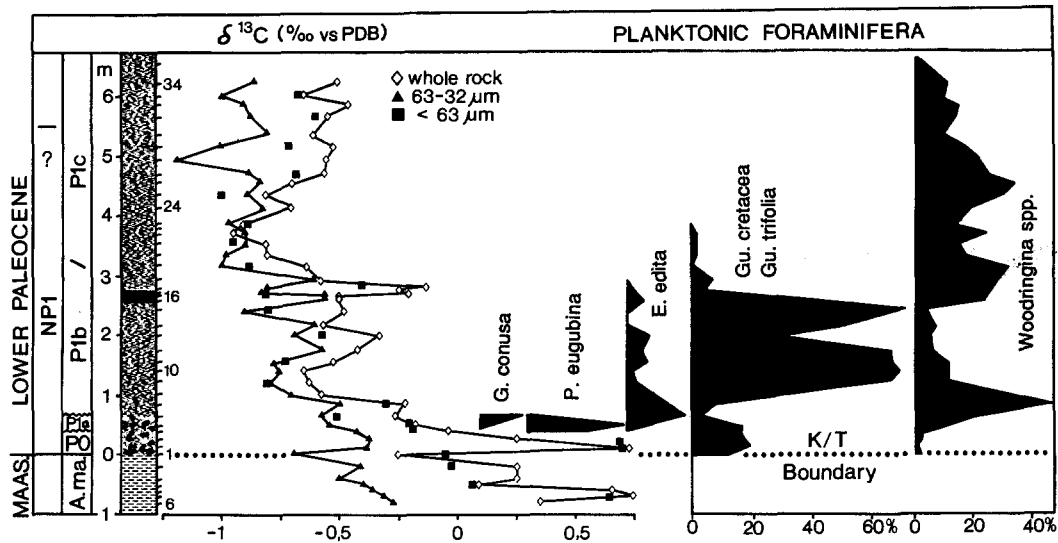


Fig.5. Detailed carbon isotopic profiles of whole rock and fine fraction and their correlation to changes in assemblages of planktic foraminifera (after Keller et al., 1990; generic assignments of planktic foraminifera follow Canudo et al., in press).

species (*Globorotalia inconstans* and *Subbotina varianta*, Keller et al., 1990).

Thus, the major characteristics of the Sinai border section $\delta^{13}\text{C}$ isotope curves are four discrete decreases in $\delta^{13}\text{C}$ values and their coincidence with abrupt changes in species dominance among planktic foraminifera. The first $\delta^{13}\text{C}$ decrease begins in the Cretaceous and culminates at the K/T boundary; the second decrease occurs near the P0/P1a boundary; the third decrease occurs just after the P1a/P1b Subzone boundary, and the fourth decrease follows a short positive $\delta^{13}\text{C}$ excursion in a thin pyrite-rich clay layer 2.6–2.7 m above the K/T boundary (Fig.5). Comparison with published $\delta^{13}\text{C}$ records shows that similar negative excursions have been observed elsewhere. For instance, a decrease in $\delta^{13}\text{C}$ values of about 1.0‰ beginning just below the K/T boundary and culminating above the boundary in Zone P1a with a further decrease in Zone P1b has also been observed in the Hor HaHar section 50 km to the east of the Negev–Sinai border section (Magaritz et al., 1985). The positive $\delta^{13}\text{C}$ excursion in the basal Danian Zone P0 was not observed, however, possibly due to wider sample spacing or the absence of Zone P0 sediments (Keller et al., 1990; Keller and Benjamini, 1991).

The $\delta^{13}\text{C}$ record of the Sinai border section is also similar to the El Kef, Tunisia isotope record although there, the decrease in ^{13}C does not begin below the K/T boundary (Keller and Lindinger, 1989). Nevertheless, there is also a rise of over 1.0‰ in $\delta^{13}\text{C}$ values in Zone P0 at El Kef followed by a drop at the P0/P1a boundary and a further decrease near the P1a/P1b boundary, similar to the Sinai border section. It appears, however, that at El Kef the $\delta^{13}\text{C}$ minima occurs near the P1a/P1b Subzone boundary (Keller and Lindinger, 1989) rather than near the P1b/P1c Subzone boundary as is the case in the Negev section.

Magaritz (1989), in his study of ^{13}C minima at major stratigraphic boundaries, reported that they are not generally found precisely at boundary horizons, but some distance above. This appears to be the case also in the K/T boundary sections in the Negev. In the Sinai border section, the minima of the $\delta^{13}\text{C}$ curve is found 3.5 m above the K/T boundary near the planktic foraminiferal Subzone P1b/P1c boundary, and in the upper part of nannofossil Zone NP1 (Fig.5). This minima is clearly seen in all three fractions analyzed. At El Kef, the ^{13}C minima is found 2.22 m above the K/T boundary near the P1a/P1b Subzone boundary. It appears therefore that although ^{13}C minima

occur some distance above boundary horizons, they are not necessarily coeval but may depend on local environmental conditions.

Oxygen isotope data

Oxygen isotope values of three sediment size fractions are illustrated in Fig.2 and Table 1. In contrast to the $\delta^{13}\text{C}$ record, the $\delta^{18}\text{O}$ record shows similar values for the two sediment fine fractions (62–32 μm , <63 μm) and a major deviation of these values from whole rock values. Moreover, the major $\delta^{18}\text{O}$ signals apparent in the fine fraction are dampened in the whole rock record. Thus, whereas whole rock variability ranges about 1.0‰ throughout the section similar to the general variability in the fine fraction, there are two major excursions of 3‰ and 4‰ in the fine fraction record which coincides with the P0/P1a boundary and the pyrite rich black clay layer at 2.6–2.7 m above the K/T boundary (Fig.2).

Figure 3 illustrates the deviation in $\delta^{18}\text{O}$ values between whole rock and the two fine fraction values. The $\delta^{18}\text{O}$ values of the w.r. samples demonstrate enrichment in ^{18}O relative to the fine fractions. As the w.r. samples also include the fine fraction, one has to conclude that the coarse fraction present in the rock is even more enriched in ^{18}O . $\delta^{18}\text{O}$ values between the w.r. and the two fine fractions range between 0.6–6‰ with the mean $\delta^{18}\text{O}$ values for w.r. – (63–32 μm) slightly larger (2.44‰) than w.r. – <63 μm (1.98‰). As noted above, the largest $\delta^{18}\text{O}$ values occur at the P0/P1a boundary and at the pyrite-rich clay layer 2.6–2.7 m above the K/T boundary.

Discussion

Identification of the source of the differences between the w.r. and fine fractions can be learned from the study of the relationship between the isotope values and the δ values (Figs.6 and 7). For $\delta^{13}\text{C}$ values a good correlation ($r=0.87$) was found between the $\delta^{13}\text{C}_{\text{w.r.}}$ and $\delta^{13}\text{C}_{\text{w.r.}-(63-32\ \mu\text{m})}$ (Fig.6). The positive correlation between the isotopic values and the fraction differential suggests that as $\delta^{13}\text{C}_{\text{w.r.}}$ values become more positive, the $\delta^{13}\text{C}_{\text{w.r.}-(63-32\ \mu\text{m})}$ increases. $\delta^{13}\text{C}_{\text{w.r.}}$ values

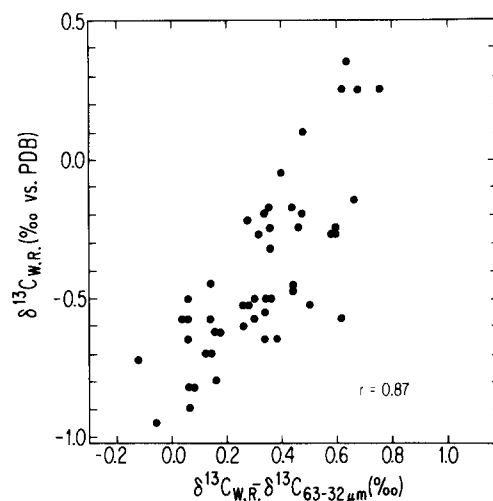


Fig.6. Correlation between $\delta^{13}\text{C}$ values of the whole rock samples and the $\delta^{13}\text{C}$ between w.r. and the 63–32 μm fraction values. The positive correlation indicates a stratigraphically dependent trend.

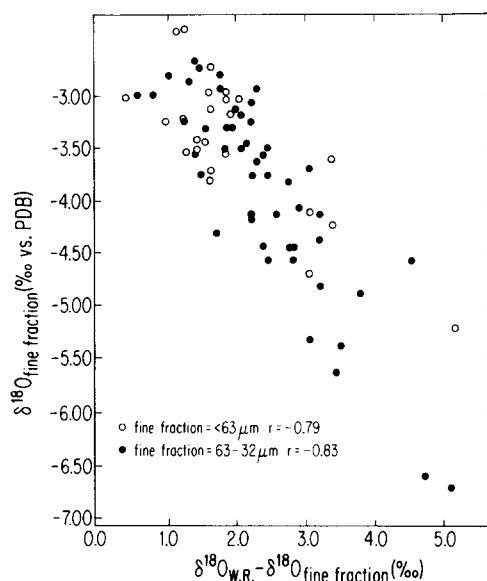


Fig.7. Correlation between the $\delta^{18}\text{O}$ values of each of the fine fractions and δ -values between the whole rock value and the two fine fractions. Large δ -values and the negative correlation indicates significant diagenetic addition of depleted ^{18}O .

become gradually more negative from the base of the section upwards (Fig.2), while $\delta^{13}\text{C}_{\text{w.r.}-(63-32\ \mu\text{m})}$ values are larger at the lower part of the section, with differences diminishing upwards. The largest δ values are found at the base of the section, and the smallest δ values in

the ^{13}C minima zone in the interval between 3–4.5 m (in the position where $\delta^{13}\text{C}_{\text{w.r.}}$ and $\delta^{13}\text{C}_{<63\ \mu\text{m}}$ show a minima, Fig.2). Some of this variation can be related to primary differences in the environment of carbonate crystallization, but the largest δ values of up to 1‰ had to reflect an addition of ^{13}C -depleted carbonate to the 63–32 μm fraction. This fraction is composed mostly of very small planktic foraminifera, and is significantly affected by carbonate cement overgrowths and infillings (Fig.4). This cement deposition seems to be quantitatively significant in this fraction only.

In Fig.7 we can demonstrate that as $\delta^{18}\text{O}_{63-32\ \mu\text{m}}$ becomes more negative, the difference between the $\delta^{18}\text{O}_{\text{w.r.}}$ and $\delta^{18}\text{O}_{63-32\ \mu\text{m}}$ values increases. Since in this case the $\delta^{18}\text{O}_{\text{w.r.}-(63-32\ \mu\text{m})}$ values reach 5‰, a late addition of CaCO_3 depleted in ^{18}O is indicated. As in the case of the $\delta^{13}\text{C}$ values, the depletion in ^{18}O in the fine fraction had to be even larger, as values of $\delta^{18}\text{O}_{\text{w.r.}}$ include also the ^{18}O depleted fraction. Note that also the data for $<63\ \mu\text{m}$ fraction show a similar trend (Fig.7).

It is important to note that in most of the samples the w.r. is enriched in both ^{18}O and ^{13}C compared to the fine fraction indicating that the best available original signal would be found in w.r. samples compared to separated fine fractions. The explanation seems to be that unsuitable biogenic CaCO_3 (e.g. aragonite, high Mg calcite) becomes redistributed locally in the host rock, particularly as spar and overgrowths in foraminiferal test interiors, and does not move far. For carbon isotopes, the $\delta^{13}\text{C}$ changes are rather small, especially for the $<63\ \mu\text{m}$ fraction (Fig.3), and one may conclude that most of these differences reflect original signals from the depositional environment. As the carbonate is composed mainly of biogenic fragments of several sources (particularly calcareous nanofossils, although many species of planktic and benthic foraminifera are present) nonequilibrium vital effects of biogenic origin may be responsible for some carbon isotopic fractionation. In addition, Fig.5 shows that $\delta^{13}\text{C}$ fluctuations operated in unison with % CaCO_3 , and with changes in planktic foraminiferal populations. This is a characteristic of the unstable productivity

conditions of the post K/T faunal recovery, with blooms of opportunistic biserial and triserial planktic foraminiferal species alternating with, and ultimately giving way to, more stable trochospiral-dominated populations (Keller and Benjamini, 1991).

This difference between the behavior of carbon vs. oxygen isotopes has clearly been demonstrated in studies of carbonate cement in carbonate terrains. The oxygen-isotope composition frequently reflects the fluid isotope composition and cementation temperature, while the carbon isotope composition of carbonate cement only slightly differs from the marine rock values (Hudson, 1975; Dickson and Coleman, 1980; Meyers and Lohmann, 1985). Even in the case of oxygen isotopes, the degree of isotopic exchange with penetrating meteoric water varies with the hydraulic conductivity of the rock unit. Limestone units that have undergone major diagenetic changes in transformation from sediment to rock, and in the course of diagenesis acted as good conduits of water are commonly depleted in ^{18}O (Magaritz, 1975). Chalks and marls, also rich in carbonate but with poorer hydraulic conductivity, generally demonstrate oxygen isotope alteration to a lesser degree.

Even carbonate units with poor conductivity can be affected significantly by diagenetic solutions in proximity to surface exposures. A systematic shift in the isotopic ratios immediately below the surface exposure was recorded by Allan and Matthews (1982). Thus the isotopic record can be used to identify near-surface events, either near to the time of sedimentation, such as early cementation, or later events of cementation and recrystallization that occurred near the surface during periods of erosion or nondeposition. In rocks in which several size fractions or types of carbonate grains are present, diagenetic solutions may affect the different fractions separately, possibly due to differential nucleation of cement crystals and differences in surface area of carbonate grains.

In our material, the isotope variations between fractions show different patterns for oxygen and carbon isotopes. The positive correlation between the $\delta^{13}\text{C}_{\text{w.r.}}$ values and $\delta^{13}\text{C}_{\text{w.r.}-(63-32\ \mu\text{m})}$ (Fig.6) and the large deviation between these two $\delta^{13}\text{C}$ values in the lowermost part of the sequence (Fig.3)

are associated with the ^{13}C enriched samples in the uppermost Maastrichtian and in Zone P0. Note that the two samples in which $\delta^{13}\text{C}_{<63\ \mu\text{m}}$ is more enriched in ^{13}C than the w.r. samples are also from the base of the P0 Zone. This pattern may reflect control of lithologic factors (grains, porosity) on the intrasample variations.

The isotopic differences between the fractions ($\delta^{18}\text{O}$) are very large and the correlation with $\delta^{18}\text{O}$ values of the fine fractions (Fig.7) indicates a significant late addition of carbonate depleted in ^{18}O . The maximal $\delta^{18}\text{O}$ values are found in specific horizons associated with stratigraphic discontinuities. Thus, the most reasonable time for addition of the diagenetic carbonates is the period of time represented by the hiatuses. Moreover, as we claim that in the fine fractions the $\delta^{18}\text{O}$ values are altered diagenetically, we can not claim that the $\delta^{18}\text{O}_{\text{w.r.}}$ reflects the original values, rather they are only closer to the original values. In some samples, $\delta^{18}\text{O}_{\text{w.r.}}$ differs by 2‰ from adjacent samples (Fig.2), and would unreasonably indicate rapid paleotemperature changes of 10°C were we to attribute the signal to environmental changes. The large fluctuations in $\delta^{18}\text{O}_{\text{w.r.}}$ values do not therefore generally reflect an original environmental signal.

We cannot attribute the fluctuations in ^{18}O to sources other than interstitial water for the following reasons: This section was (a) never buried beneath more than a few hundred meters of marine and continental sediment; (b) was never significantly elevated above ambient ground water temperatures; (c) there is no evidence for passage of hydrothermal water, and (d) it is not located in a tectonically or volcanically active area. Therefore the possibility of water release from other sources, such as deep waters of hydrothermal origin or altered clay minerals does not arise. In any case, interstitial ^{18}O -depleted fluids generated by sources such as these would result in a more homogeneous contribution of low ^{18}O carbonate.

The interval from 2.6 to 3 m, associated with the black pyrite-rich clay layer, is the part of the section most depleted in ^{18}O , in particular the 63–32 μm fraction (Figs.2 and 3). Such pyrite concentrations in marine sediments usually represent pyrite replacement of organic matter. Enrich-

ment in organic matter together with ^{18}O depletion has been used as an indication of sapropelic environmental conditions in the Eastern Mediterranean during the Neogene (Thunnell et al., 1984). The similarity of this early Tertiary event in the Negev to some aspects of the Mediterranean Sea Neogene sediments may suggest a brief sapropelic episode in this part of the Tethys ocean during the early Tertiary.

Although the original depositional oxygen isotope signal seems to have been mostly destroyed, the data can be used to study the diagenetic history of the section. As very large changes in $\delta^{18}\text{O}$ (Fig.3) are found between nearby samples, the addition of ^{18}O depleted carbonate is not homogeneously distributed along the section. The samples which have large $\delta^{18}\text{O}$ values can be correlated with transitions in the faunal record as presented by Keller et al. (1990) and Keller and Benjamini (1991). Two intervals of ^{18}O depletion will be discussed.

(1) At 50 cm above the K/T boundary. The maximal $\delta^{18}\text{O}$ samples occur at the planktic foraminiferal subzone transition P0/P1a. The estimated duration of Zone P0 is 50,000 years and of Subzone P1a, 180,000 years (Berggren et al., 1985). The sediment thickness in the Negev for this interval is significantly less than at El Kef, Tunisia (50 cm as compared to 3 m, Keller, 1988). The argument for a hiatus at this position in the Negev is based on the abrupt termination of the ranges of *Parvularugoglobigerina eugubina* and *Globastica conusa* suggesting that the top of Subzone P1a is missing (Fig.5). Evidence for a short sea level regression at this time during a generally transgressive sea comes also from the El Kef, Tunisia, and Brazos River, Texas, sections. At the latter locality, grey clay sediments containing planktic faunas similar to the eastern Negev are truncated by a sandy, glauconite-rich horizon indicating submarine erosion (Keller, 1989a).

(2) At the interval between 2.6–2.7 m in the upper part of Subzone P1b, associated with the black pyrite rich clay layer. This layer has at its base a reddish iron-rich layer which may also indicate non-deposition or a hiatus, but the cause of the depletion in w.r. ^{18}O may be an initial signal

derived from the sapropelic conditions as discussed above.

Occurrences of $\delta^{18}\text{O}$ peaks at the subzone boundary and the black pyrite-rich clay layer may suggest that at the time of these transitions, environmental changes were taking place which subtly affected both the sedimentary and fossil records simultaneously. The effects may be observed only when both the sediments and fossil populations are scrutinized closely, as illustrated in Fig.2. The local sedimentary reflection of the environmental perturbations includes not only erosion and dissolution, but also addition of secondary calcite (Fig.4) to the layers below the surface. As the thickness of the ^{18}O depleted zones are small, short-duration events affecting only a thin surface zone are indicated, unlike the major unconformities discussed by Allan and Matthews (1982), where the ^{18}O depleted zone can extend several meters. The depletion in ^{18}O at these horizons suggests meteoric water rather than seawater cementation. Again we would like to mention that as the 63–32 μm carbonate fraction still contains original marine carbonate test material, the added calcite had to be even more depleted in ^{18}O than the most depleted sample (-6.7%) for this fraction. However, since the benthic foraminiferal evidence indicates that deposition took place at outer neritic or upper slope depths (200–300 m), the isotopic effects observed seem to be due to post-depositional alterations connected with conductivity of meteoric waters at this horizon. Evidence for meteoric water is not in all cases indication for emergence. In recent marine sediments on continental slopes, evidence for meteoric water flow exists wherever samples were taken (Essaid, 1988; Leahy and Meisler, 1988).

Some of the features of the carbon isotope record can also be integrated into this environmental picture. The minima of $\delta^{13}\text{C}$ values at 0.5–0.7 m for both the w.r. and $<63\ \mu\text{m}$ fractions correlate with the large percentage increase in benthic foraminifera at this interval (Keller et al., 1990). The maxima of $\delta^{13}\text{C}_{\text{w.r.}}$ at 3 m height (Fig.5) correlates with the large $\delta^{18}\text{O}$ values associated with the dark clay layer. Note that while $\delta^{13}\text{C}_{\text{w.r.} - <63\ \mu\text{m}}$ values change gradually at this

interval, $\delta^{13}\text{C}_{\text{w.r.} - (63-32\ \mu\text{m})}$ changes rapidly from almost 0‰ to 0.7‰ (Fig.3).

One of the significant characteristics of $\delta^{13}\text{C}$ curves at major Phanerozoic boundary horizons is the identification of the minima associated with boundary extinctions (Magaritz, 1989). As can be seen in our profile (Fig.2), the minima in the $\delta^{13}\text{C}$ curve occurs at 3–3.5 m and thus several meters of section is present between the beginning of the drop in ^{13}C and the minima. Earlier, this minima was dated at 200,000 years after the boundary event at South Atlantic site 527 (Shackleton and Hall, 1984) and occurs at about the equivalent biostratigraphic position (upper Zone P1a) at El Kef, Tunisia (Keller and Lindinger, 1989). The minima zone found in the Sinai border sections occurs later, in the upper part of the NP1 nannofossil zone, and at the base of planktic foraminiferal Subzone P1c, and just below the onset of stable carbonate deposition after the K/T boundary event in the Negev (Keller et al., 1990). This supports the Magaritz (1989) model, in that the carbon isotope record reflects major changes in *total* biomass, and is composed of several components.

(a) The decline associated with the boundary beginning below the K/T boundary (Magaritz et al., 1985) and extending approximately 4 m above the boundary.

(b) The minimum, which occurs several 10^5 years later, at 4–5 m above the K/T boundary.

(c) Recovery of the biological system from about 5 m upsection reflecting an increase of both $\delta^{13}\text{C}$ values and carbonate percentage (Keller et al., 1990).

The NP1/NP2 nannofossil boundary at 5.5 m marks the time when carbonate deposition reached stable levels, and marks the end of the period of fast recovery of $\delta^{13}\text{C}$ values (Fig.2). At this level, mass appearance of Tertiary calcareous nannoplankton indicates stabilization of the marine planktic ecosystem (Keller et al., 1990). According to the time scale of Berggren et al. (1985) stabilization occurred 400,000 years following the K/T extinction. As the planktic foraminiferal subzone transition P1a/P1b occurs near the magnetic reversal C29R to C29N, some 230,000 years after the K/T event, and the $\delta^{13}\text{C}$ minima is reached only

near the base of Subzone P1c, stabilization of the marine ecosystem in the eastern Tethys appears to have occurred between 300,000 and 400,000 years after the K/T boundary event. The minima zone of the $\delta^{13}\text{C}$ curve can be identified both in the w.r. samples and the two fine fractions (Fig.2); it is also the zone with minimal $\delta^{13}\text{C}$ (Fig.3), indicating that it, at least, is unaffected by diagenetic overprints.

Conclusions

The interpretation of our isotopic data suggests that in the eastern Tethys the lowermost Tertiary biozone transitions are associated with zones of diagenetic alteration of the type caused by surface exposure to meteoric water either at the land surface, or in the submarine environment influenced by the meteoric water. Since benthic, foraminifera indicate deposition in relatively deep water (200–300 m depth), uplift and subaerial exposure contributing to the isotope shift must have taken place in the post-depositional period. On the other hand, if the meteoric water is associated with submarine flow, the zones of large ^{18}O depletion may be correlated to periods of flow changes in the interstitial solution in the shelf sediments at times of sea level changes. The main intervals of alteration underlie sedimentary hiatuses as determined by abrupt changes in planktic foraminiferal populations (Keller et al. 1990). Some of the hiatuses are marked by influx of ^{18}O depleted water. In one case, the changes are better explained by variations in productivity and/or fresh water influx into the marine environment. In general, the global post-K/T decrease in carbonate productivity occurring in the interval from the latest Maastrichtian to the base of planktic foraminiferal Subzone P1c, as determined both by CaCO_3 depositional rates and by marine carbonate ^{13}C depletion, can also be traced in the studied section in the Negev. Similarly, the global productivity increase can be observed in nannozone NP2, associated with an increase in CaCO_3 content and ^{13}C content of DIC; although at this time $\delta^{13}\text{C}$ values do not reach Maastrichtian levels.

Acknowledgements

The authors thank R. Salnikow and K. Bijan (of W.I.S.) for isotope measurements, M. Dvoraček (G.S.I.) for SEM work. This research was supported by grant No. 86-00110 from the United States – Israel Binational Science Foundation (BSF), Jerusalem, Israel, to C. Benjamini and G. Keller and NSF grant OCE 8811732 to G. Keller. Contribution no. 10 of the Department of Environmental Sciences and Energy Research, the Weizmann Institute of Science.

References

- Allan, J. R. and Matthews, R. K., 1982. Isotope signatures associated with early meteoric diagenesis. *Sedimentology*, 29: 797–817.
- Arkin, Y., Nathan, Y. and Starinsky, A., 1972. Paleocene–Early Eocene environments of deposition in the northern Negev (southern Israel). *Geol. Surv. Israel Bull.*, 56, 18 pp.
- Berggren, W. A., Kent, D. V. and Flynn, J. J., 1985. Jurassic to Paleogene: Part 2, Paleogene geochronology and chronostratigraphy. In: N. J. Snelling (Editor), *The Chronology of the Geologic Record*. *Geol. Soc. Lond. Mem.*, 10: 141–195.
- Canudo, J. I., 1990. Los Foraminiferos planctonicos del Paleoceno–Eoceno en el Prepirineo Meridional y su Comparacion con la Cordillera Betica. Thesis. Univ. Zaragoza, 435 pp. (unpublished).
- Canudo, J. I., Keller, G. and Molina, E., in press. Cretaceous–Tertiary Boundary extinction pattern and faunal turnover at Agost and Caravaca, SE Spain. *Mar. Micropaleontol.*
- Dickson, J. A. D. and Coleman, M. L., 1980. Changes in carbon and oxygen isotopic composition during limestone diagenesis. *Sedimentology*, 27: 107–118.
- Essaid, H. I., 1988. Response of a layered control aquifer to sea level changes. *EOS*, 69: 356.
- Hudson, J. D., 1975. Carbon isotopes and limestone cement. *Geology*, 3: 19–22.
- Keller, G., 1988. Extinction, survivorship and evolution of planktic foraminifera across the Cretaceous/Tertiary boundary at El Kef, Tunisia. *Mar. Micropaleontol.*, 13: 239–263.
- Keller, G., 1989a. Extended Cretaceous/Tertiary boundary extinctions and delayed population change in planktic foraminifera from Brazos River, Texas. *Paleoceanography*, 4(3): 287–332.
- Keller, G., 1989b. Extended period of extinctions across the Cretaceous/Tertiary boundary in planktic foraminifera of Continental-shelf sections: Implications for impact and volcanism theories. *Geol. Soc. Am. Bull.*, 101: 1408–1418.
- Keller, G., 1990. Paleoecologic response of Tethyan benthic foraminifera to the Cretaceous–Tertiary transition. *Proc. 4th. Int. Symp. Benthic Foraminifera*.
- Keller, G., Benjamini, C., Magaritz, M. and Moshkovitz, S., 1990. Faunal, erosional and CaCO_3 events in the early

- Tertiary eastern Tethys. *Geol. Soc. Am., Spec. Pap.*, 24: 471–480.
- Keller, G. and Benjamini, C., 1991. Paleoenvironment of the eastern Tethys in the Early Paleocene. *Palaios*.
- Keller, G. and Lindinger, M., 1989. Stable isotope, TOC, and CaCO₃ records across the Cretaceous/Tertiary boundary at El Kef, Tunisia. *Palaeogeogr., Palaeoclimatol., Palaeoecol.*, 73: 243–265.
- Leahy, P. P. and Meisler, H., 1988. Effect of eustatic sea level changes in the position of salt water–fresh water transition zone in the coastal plain aquifer of New Jersey. *EOS*, 69: 356.
- Magaritz, M., 1975. Sparitization of a pelleted limestone: A case study of carbon and oxygen isotopic composition. *J. Sediment. Petrol.*, 45: 599–603.
- Magaritz, M., 1963. Carbon and oxygen isotope composition of recent and ancient coated grains. In: T. M. Peryt (Editor), *Coated Grains*. Springer, Berlin, pp. 27–37.
- Magaritz, M., 1989. ¹³C minima follow extinction events: A clue to faunal radiation. *Geology*, 17: 337–340.
- Magaritz, M., Moshkovitz, S., Benjamini, C., Hansen, H. J., Hakansson, E. and Rasmussen, K. L., 1985. Carbon isotope-, bio- and magnetostratigraphy across the Cretaceous–Tertiary boundary in the Zin Valley, Negev, Israel. *Newsl. Stratigr.*, 15(2): 100–113.
- Meyers, W. J. and Lohmann, K. C., 1985. Isotope geochemistry of regionally extensive calcite cement zones and marine components in Mississippian limestones, New Mexico. In: N. Schneidermann and D. M. Harris (Editors), *Carbonate Cements*. *SEPM Spec. Publ.*, 36: 223–239.
- Nathan, Y., 1966. Studies of palygorskite. Thesis. Hebrew Univ., Jerusalem.
- Paull, C. K. and Thierstein, H. R., 1987. Stable isotopic fractionation among particles in Quaternary coccolith-sized deep-sea sediments. *Paleoceanography*, 2(4): 423–429.
- Perch-Nielsen, K., McKenzie, J. and He, Q., 1982. Biostratigraphy and isotope stratigraphy and the 'catastrophic' extinction of calcareous nannoplankton at the Cretaceous/Tertiary boundary. *Geol. Soc. Am., Spec. Pap.*, 190: 353–371.
- Shackleton, N. J. and Hall, M. A., 1984. Carbon isotope data from Leg 74 sediments. In: *Initial Rep. DSDP*, 74: 613–619.
- Smit, J., 1982. Extinction and evolution of planktonic foraminifera after a major impact at the Cretaceous/Tertiary boundary. *Geol. Soc. Am., Spec. Pap.*, 190: 329–352.
- Stott, L. D. and Kennett, J. P., 1989. New constraints on early Tertiary paleoproductivity from carbon isotopes in foraminifera. *Nature*, 342: 526–529.
- Thunell, R. C., Williams, F. D. and Belyea, P. R., 1984. Anoxic events in the Mediterranean Sea in relation to the evolution of Late Neogene climates. *Mar. Geol.*, 59: 105–134.
- Zachos, J. C. and Arthur, M. A., 1986. Paleoceanography of the Cretaceous/Tertiary boundary event: Inferences from stable isotopic and other data. *Paleoceanography*, 1: 563–602.